THE JOURNAL OF PROSTHETIC DENTISTRY

RESEARCH AND EDUCATION

Bond strengths of porcelain to cobalt-chromium alloys made by casting, milling, and selective laser melting

Jieyin Li, DDS,[a] Chaojie Chen, DDS,[b] Juankun Liao, DDS,[c] Lang Liu, DDS,[d] Xiuhua Ye, DDS,[e] Shiyao Lin, DDS,[f] and Jiantao Ye, DDS, MD[g]

ABSTRACT

Statement of problem. Cobalt-chromium (Co-Cr) alloys have been widely used for metal-ceramic fixed prostheses and can be fabricated using conventionally cast or new computer-aided technology. However, the effect of different manufacturing methods on the metal-ceramic bond strength needs further evaluation.

Purpose. The purpose of this in vitro study was to evaluate the metal-ceramic bond strength of a Co-Cr alloy made by casting, milling, and selective laser melting (SLM).

Material and methods. Co-Cr specimens (25×3×0.5 mm) were prepared using a cast, milled, or SLM method and layered with ceramic (8×3×1.1 mm). Metal-ceramic bond strength was measured by a 3-point bend test according to ISO9693. The area fraction of adherence porcelain (AFAP) was determined by measuring the Si content of the specimens with scanning electron microscopy/energy dispersive spectroscopy (SEM/EDS). The metal-ceramic bond strength and AFAP results were analyzed using 1-way analysis of variance and the Bonferroni post hoc test (α=.05). SEM/EDS and metallurgic microscopy were also used to study the specimens' morphology, elemental composition, and metallurgic structure.

Results. No significant differences (P>.05) were found for the bond strength among cast, milled, and SLM Co-Cr alloys. The milled and SLM groups showed significantly more porcelain adherence than the cast group (P<.001). The surface morphologies and oxidation characters of cast, milled, and SLM Co-Cr alloys were similar, whereas the metallurgic structures were different.

Conclusions. The bond strength between ceramics and Co-Cr alloys is independent of the manufacturing method. However, milling- and SLM-produced alloys had better porcelain adherence. (J Prosthet Dent 2017;118:69-75)

For decades, metal-ceramic prostheses have provided good performance and esthetics.[1] The metal frameworks of metal-ceramic prostheses are often made with Co-Cr alloys with excellent clinical success.[2] Making a framework for a prosthesis by casting requires much time and labor and has various disadvantages including distortion of wax patterns and irregularities in the cast metal. However, recent advances have allowed restorations to be fabricated with a variety of computer-aided technologies.[3] These technologies can be broadly divided into 2 categories: computer-aided design and computer-aided manufacture (CAD-CAM) milling and selective laser melting (SLM). These techniques have eliminated the time-consuming casting process and human error.[4,5]

SLM is an additive manufacturing process that produces metal components from a 3-dimensional (3D) CAD cast by fusing fine layers of metal powder with a focused high-power laser beam.[3] SLM can produce metal with high dimensional accuracy and up to 100% density.[6] CAD-CAM milling uses tools to mill or grind restorations or frameworks from solid blocks of material and can

J.L. and C.C. contributed equally to this work.
[a]Resident, Department of Stomatology, Jieyang People's Hospital, Jieyang, PR China.
[b]Technical director, Dingyuan Dental Lab, Ltd, Dongguan, PR China.
[c]Resident, Department of Prosthodontics, Sun Yat-Sen Memorial Hospital, Sun Yat-Sen University, Guangzhou, PR China.
[d]Resident, Department of Prosthodontics, Sun Yat-Sen Memorial Hospital, Sun Yat-Sen University, Guangzhou, PR China.
[e]Resident, Department of Prosthodontics, Sun Yat-Sen Memorial Hospital, Sun Yat-Sen University, Guangzhou, PR China.
[f]Resident, Department of Prosthodontics, Sun Yat-Sen Memorial Hospital, Sun Yat-Sen University, Guangzhou, PR China.
[g]Assistant Professor and Director, Department of Prosthodontics, Sun Yat-sen Memorial Hospital, Sun Yat-sen University, Guangzhou, PR China.

Clinical Implications

The metal-ceramic bond strength of Co-Cr alloy is independent of the manufacturing method. Milling and SLM may eventually replace casting for the production of Co-Cr frameworks.

process many different materials, including titanium, ceramics, and Co-Cr alloys, suitable for processing on smaller computer numerical control mills.[7,8] CAD-CAM milling eliminates the flaws and porosity induced by casting because blanks can be made under highly standardized industrial conditions.[9] Cobalt-chromium alloys have been widely used in CAM-CAM milling and SLM technologies because their biocompatibility is better than that of nickel-chromium alloys.[10] Although these methods show promise for fabricating prostheses, they must be tested in both the laboratory and the clinic to ensure that they produce dental restorations of a quality at least equal to those produced by conventional techniques. Important properties include acceptable biocompatibility, good corrosion resistance, low internal porosity, adequate mechanical properties, good marginal fit, and adequate bond strength to porcelain.[11-16]

The clinical success of a metal-ceramic restoration depends primarily on the bond strength between the porcelain and the metal substructure.[17] Metal-ceramic bonding appears to result from chemical bonding, mechanical interlocking, van der Waals forces, and compressive bonding, although among these, chemical bonding dominates.[18] Chemical bonding with metal can change when an oxide layer forms on its surface.[19] Thus, to understand chemical bonding to an alloy, its morphology, oxide layer, and metal-ceramic interface must be studied. Although studies have evaluated the bond strength of dental porcelain to cast, milled, and SLM Co-Cr alloy,[12,20,21] the characterization of the oxidation of the metal surfaces, matrix structure, and interface combination status has been lacking. Therefore, because metal-ceramic restorations continue to be used and because new fabrication technologies are being developed, the purpose of this paper was to compare the metal-ceramic bond strengths, the metallurgic structures before and after firing, and the surface and interfacial characteristics of Co-Cr alloys made by casting, milling, and SLM. The null hypothesis was that the bond strength and area fraction of adherence porcelain (AFAP) would be independent of manufacturing method.

MATERIAL AND METHODS

To make the cast Co-Cr alloy specimens, a 3D modeler (Projet-DP 3000; 3D Systems) was used to create 11 acrylic resin templates (VisiJet CP200; 3D Systems) with dimensions of 25×3×0.5 mm, according to ISO9693 standard.[22] Eleven specimens of the Co-Cr alloys (Wirobond 280; Bego; Co, 60.2%; Cr, 25.0%; Mo, 4.8%; W, 6.2%; Ga, 2.9%; Si, <1.0%; Mn, <1.0%) were cast in an electrical induction furnace (Nautilus; Bego) according to the manufacturer's recommendations.

Eleven milled metal disks (25×3×0.5 mm) were made from solid blanks (ET-02, Echt TEC; Co, 62.0%; Cr, 25.0%; Mo, 6.0%; W, 5.0%; Si, 1.0%; Nb, 1.0%) with a computer numerical control mill (HA-5AX2; SFY Co) according to the manufacturer's instructions. Eleven metal specimens (25×3×0.5 mm) were produced by SLM. Their designs were produced in CAD (PowerSHAPE; Delcam) and converted to standard tessellation language files, which were transmitted to the SLM equipment (Mlab cusing; Concept Laser). This SLM equipment sintered the Co-Cr powder (Wirobond C^+; Bego; Co, 63.9%; Cr, 24.7%; Mo, 5%; W, 5.4%; Si, <1%). SLM specifications were based on the standard method recommended by the manufacturer. The scan speed was 7 m/s, the lamination thickness was 25 μm, the power of the Yb-fiber laser was 100 W, and the fabrication speed was 5 cm^3/h.

The dimensions of all specimens were confirmed with a 0.02-mm precision digital caliper (Hengliang); all specimens met ISO9693 standard.[22] The specimens were then ground and airborne-particle abraded for 10 seconds at a pressure of 0.2 MPa, using 125-μm Al_2O_3 particles at an angle of 45 degrees from a distance of approximately 1 cm. The specimens were then placed in a programmable dental porcelain furnace (Programat P300; Ivoclar Vivadent AG) at a vacuum level of 0.0036 MPa, heated from 600°C to 980°C at 50°C min^{-1} and then held at the peak temperature for 2 minutes.

A ceramic layer (Ceramco III; Dentsply Sirona) (8×3×1.1 mm) was applied on the center of each metal specimen. This porcelain was fired in a furnace (Programat P300; Ivoclar Vivadent AG) according to the manufacturer's recommendations. From each group of 11 specimens, with simple random sampling method, 1 random specimen was selected for a study of interface morphology. These specimens were embedded in phenolic resin (Weiyi), longitudinally sectioned, ground and polished, and then ultrasonically cleaned, dried, and sprayed with carbon powder to prepare for observation by scanning electron microscopy (SEM; JCX8100; JEOL).

The bond strength levels of the metal-ceramic specimens of each group (n=10) were measured using a 3-point bend test in a universal testing machine (Sans) with a 100-N load cell according to ISO9693 standard.[22] The bond strength, τ_b, for each specimen was calculated using the equation [$\tau_b = k \times F_{fail}$], where coefficient k is a function of the elastic modulus (Wirobond 280: 220 GPa, Wirobond C^+: 210 GPa, ET-02: 190 GPa) of the metal used and its thickness, and F_{fail} is the load at failure.

All fractured specimens were observed with the naked eye, and representative images were made using a digital camera. The types of bond failure were classified as adhesive (failure between the metal and the porcelain), cohesive (failure entirely within the porcelain), or mixed mode (a combination of adhesive and cohesive failure).[23] To quantify the AFAP, 10 specimens from each group were analyzed using an SEM equipped with energy-dispersive x-ray spectroscopy (EDS; Oxford-7412; Oxford Instruments). The EDS was rastered over the central part of the specimens at ×40 magnification using a Si x-ray detector after performing the oxidation heat treatment, after applying opaque porcelain, and after debonding the porcelain from the metal bar. The AFAP was estimated as $AFAP=(Si_f - Si_m)/(Si_o - Si_m)$, where Si_f is the atomic percentage of silicon on the surface after porcelain fracture, Si_o is the atomic percentage of silicon on the surface after firing the opaque porcelain, and Si_m is the atomic percentage of silicon on the oxidized metal surface before applying the porcelain.[24] Quantitative analysis of the acquired spectra was conducted using software (INCA Suite v4.13) in a nonstandard analysis.

To study the oxidation and metallurgic structure of the 3 Co-Cr alloys, 17 additional cast, milled, and SLM Co-Cr alloys were fabricated in the same way. SEM/EDS was used to analyze the surface morphology and elemental composition of 5 specimens from each group with simple random sampling method after airborne-particle abrasion with Al_2O_3, after oxidation heat treatment, and after the firing cycle for opaque porcelain. The EDS analysis was conducted on the central part (8×3 mm) of the surface at ×40 magnification. The EDS had a detector window made from silicon (lithium [Si Li]), its accelerating voltage was 20 kV, and its specimen working distance was 11 mm. This analysis was performed with ZAF correction, correcting the Z number, absorption (A), and fluorescence (F). Using metallurgic microscopy (DM4000; Leica), the metallurgic structure of 1 specimen from each group was observed after airborne-particle abrasion with Al_2O_3, and after the firing cycle for opaque and dentin porcelain. Before observation, the specimens were polished and then etched in a mixture of hydrofluoric/nitric/hydrochloric acid for 30 seconds.

Data were evaluated using software (PASW Statistics v16.0; SPSS Inc). The bond strength and AFAP results were analyzed using 1-way analysis of variance (ANOVA), followed by the Bonferroni post hoc test (α=.05).

RESULTS

The mean bond strength and standard deviations for the 3 groups are shown in Table 1. One-way ANOVA showed no significant differences among the 3 groups (df=2, F =1.079, P=.354).

Table 1. Bond strength values of cast, milled, and SLM groups

Group	n	Mean ±SD[a]
Cast	10	32.15 ±2.39[a]
Milled	10	33.96 ±4.40[a]
SLM	10	32.31 ±3.06[a]

SLM, selective laser melting. [a]Groups with same superscripted letters not significantly different at α=.05.

The 3 groups of Co-Cr alloys showed no obvious differences in surface morphology, both after airborne-particle abrasion and after heat treatment. After airborne-particle abrasion, the surfaces exhibited sharp edges and undercuts. After heat treatment, the sharp edges and undercuts were smoothed by sagging. SEM images of the metal-ceramic interfaces (Fig. 1) showed 3 distinct regions: ceramic substrate, metal-ceramic interaction zone, and metal substrate. The interfaces were intact, with good contact between the ceramic and Co-Cr alloy and with no cracks or holes.

Table 2 shows the mean compositions of 5 specimens from each of the 3 groups of Co-Cr alloys after each of the 3 surface preparation stages. At the same preparation stage, the 3 groups show similar surface compositions. After airborne-particle abrasion, the surfaces of all 3 groups exhibited aluminum (Al) and oxygen (O), which were not present in the batch composition. After heat treatment, the O and Cr contents increased and the Co content decreased, whereas the Si, Mo, and W contents did not differ noticeably compared with those after airborne-particle abrasion. After the simulated opaque firing, the surface compositions showed no distinct changes from those after the heat treatment.

Figure 2 shows the metallurgic structure of the Co-Cr alloys fabricated with casting, milling, or SLM. In the same group of Co-Cr alloys, the metallurgic structure was not noticeably different between before heat treatment and after simulated porcelain firing, but the metallurgic structures were noticeably different among the Co-Cr alloys fabricated by different methods. The cast and milled specimen mainly consisted of austenitic matrix and carbide. The carbide content was enriched along the grain boundaries with a typical dendritic-like morphology in the cast specimen (Fig. 2A, B) and an island-shaped morphology in the milled specimen (Fig. 2C, D); the milled alloy also had a precipitated phase with a particle shape (Fig. 2C, D). In contrast, the SLM alloy showed an austenitic matrix with fine grains, without an obvious precipitated phase (Fig. 2E, F).

To the naked eye, all the specimens appeared to have an area where the ceramic was completely removed and other areas where a thin layer of ceramic remained adhered. Thus, all 3 groups of specimens exhibited a mixture of adhesive and cohesive failure (Fig. 3). Table 3 shows the quantitative AFAP values. One-way ANOVA revealed significant differences among the groups

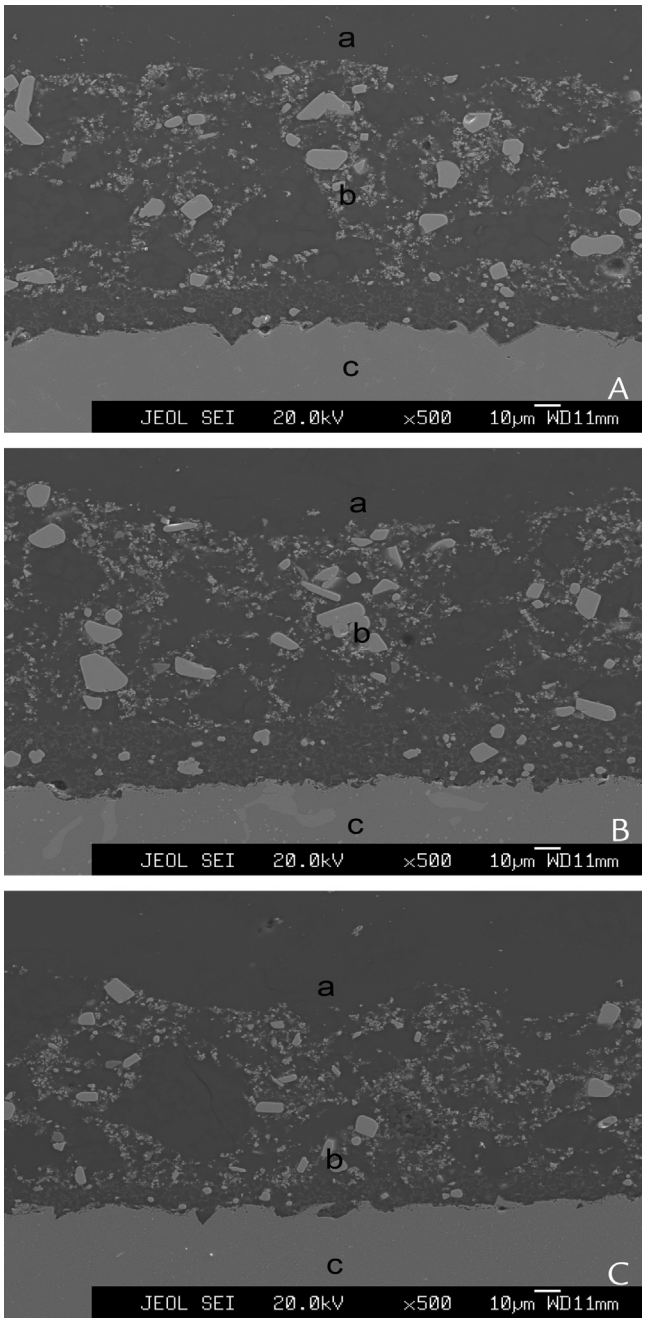

Figure 1. Interface of metal-ceramic specimens (original magnification ×500). A, Cast. B, Milled. C, Selective laser melted. (a) Ceramic substrate; (b) metal-ceramic interaction zone; and (c) metal substrate.

(*df*=2, *F*=39. 989, *P*<.001). The Bonferroni post hoc test revealed significant differences between groups (*P*<.001), except between the milled and SLM groups (*P*=0.61).

DISCUSSION

This study evaluated the metal-ceramic bond strength and AFAP of a Co-Cr alloy made by using different techniques. No significant differences were observed among the 3 groups regarding metal-ceramic bond strength, so the null hypothesis was accepted. The milled and SLM groups showed significantly more porcelain adherence than the cast group, so the null hypothesis was rejected.

Table 2. Mean values for elemental concentrations[a]

Group	Preparation Stage	O	Al	Co	Cr	Mo	W
Cast	Airborne-particle abrasion	7	11	51	21	4	5
	Heating	23	9	28	31	4	4
	Simulated opaque firing	23	8	28	34	3	3
Milled	Airborne-particle abrasion	7	10	51	21	4	5
	Heating	22	8	30	32	3	4
	Simulated opaque firing	23	7	29	35	3	4
SLM	Airborne-particle abrasion	7	11	52	22	5	4
	Heating	24	8	28	34	3	3
	Simulated opaque firing	24	6	26	37	4	3

[a]Mean values shown for elemental concentrations (by wt %) of cast, milled, and selective laser melting (SLM) Co-Cr alloys for 3 preparation stages (n=5).

Chemical bonding to an alloy surface changes in the presence of metal oxides. Heating a metal before applying it to porcelain can create surface oxides that improve chemical bonding.[25] The 3 groups of Co-Cr alloys tested had similar surface oxides during the same preparation stage, and they changed similarly as preparation progressed. After heat treatment, the O and Cr content of all 3 groups sharply increased, suggesting that oxides had formed on the surface. Wylie et al[26] found that a successive Cr_2O_3 oxide layer can form when the Cr content in an alloy reaches 20%. Wu et al[27] also found that, with Co-Cr alloys, mostly chromium oxides migrated into the ceramic layer and formed chemical bonds. Johnson et al[28] found a reducing Ni and increasing Cr, O contents on Ni-Cr alloy surface after heat treatment and simulated opaque firing, and Cr appear in the form of CrO_2, Cr_2O_3. Thus, in our study, we believe that predominantly chromium oxides formed on the surfaces and participated in chemical bonding after heat treatment. After heat treatment, the 3 groups showed similar O and Cr concentrations. After simulated opaque firing, the O concentration did not increase noticeably, suggesting that the alloys had oxidized only slightly and that the oxidation characteristics of the 3 Co-Cr alloys were similar. Johnson et al[28] reported different results for a Ni-Cr alloy, finding that its surface oxygen concentration increased after simulated opaque firing, which suggests that its surface continued to oxidize. These differences may result from differences in the alloy type and the holding time at the peak temperature during opaque porcelain firing.

Different manufacturing methods may result in different alloy morphologies and change the nature of the surface oxides, thereby affecting the metal-ceramic bond strength.[20] Our results show that the metal-ceramic bond strength was independent of the Co-Cr manufacturing method. This result is probably because after airborne-particle abrasion with 125-μm Al_2O_3 the 3 Co-Cr alloys had similar morphologies and because after

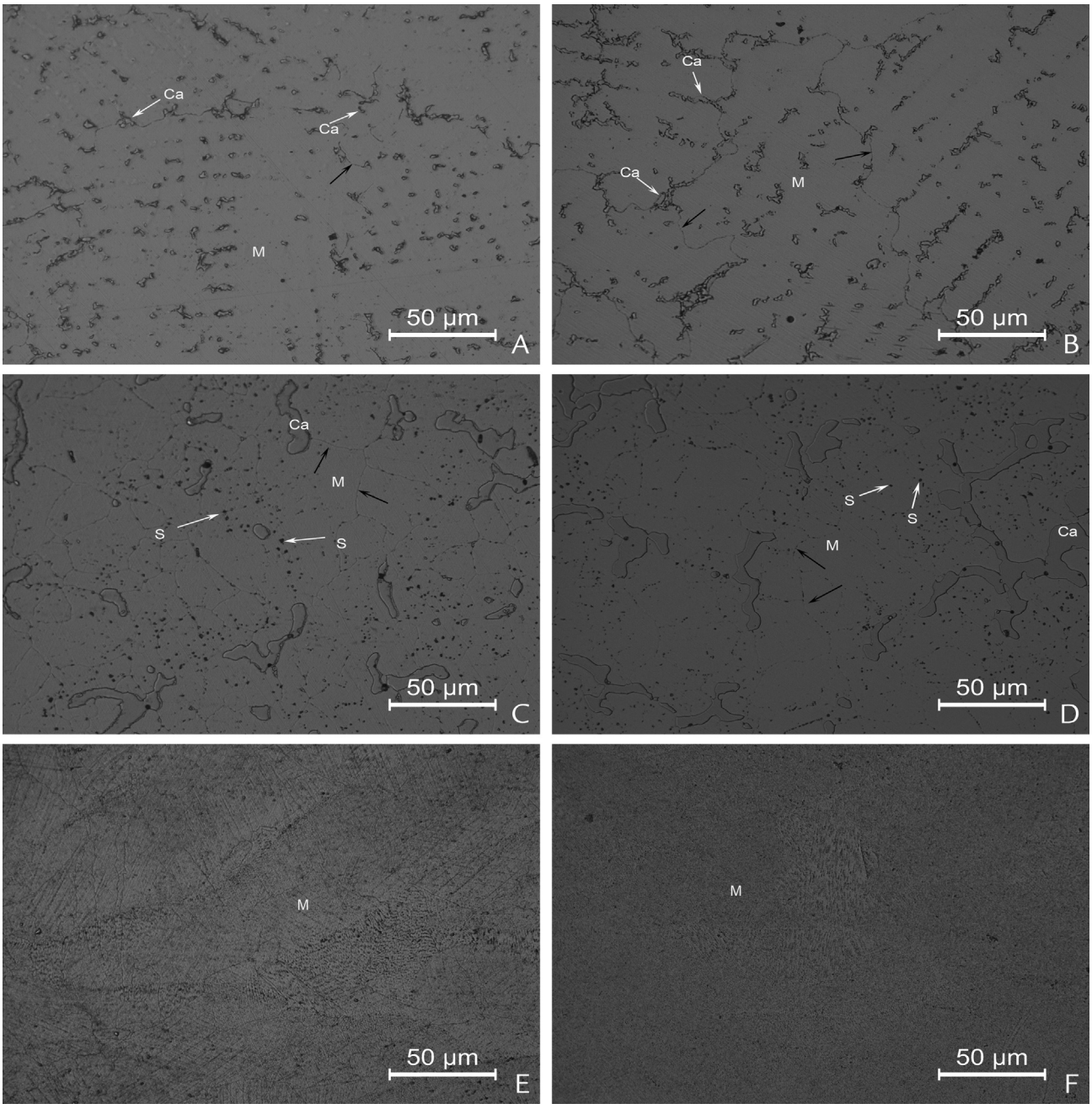

Figure 2. Metallurgic structure of Co-Cr alloy. A, Cast specimen before heat treatment. B, Cast specimen after simulated porcelain firing. C, Milled specimen before heat treatment. D, Milled specimen after simulated porcelain firing. E, SLM specimen before heat treatment. F, SLM specimen after simulated porcelain firing. Ca, carbide; M, austenitic matrix; S, precipitated phase with particle shape (black arrows show grain boundaries); SLM, selective laser melted.

heat treatment they had similar oxidation properties, resulting in similar mechanical and chemical bonds. Further research is needed to confirm the optimum thickness of the oxide layer obtained from different manufacturing methods. Serra-Prat et al[20] compared the metal-ceramic bonds of Co-Cr alloys fabricated using casting, milling, and SLM and found no significant differences; this is consistent with our study. Xiang et al[12] and Akova et al[29] found no differences between the metal-ceramic bond strength of cast and milled Co-Cr alloys. Lee et al[30] reported no differences in the metal-ceramic bond strengths of Co-Cr alloys fabricated using casting and milling. These results were also similar to ours. In contrast, Bae et al[21] considered that the metal-ceramic bond strength of SLM Co-Cr alloys could be improved by the lamellar morphology of the alloy

Figure 3. Fractured specimens. A, Cast. B, Milled. C, Selective laser melted.

surface. In their study, after airborne-particle abrasion with 50-μm Al_2O_3, the SLM Co-Cr alloy surface exhibited 100-μm-thick layers aligned with the laser irradiation, and a gap was seen between the layers. They believed that the metal-ceramic bond strength increased because of the ceramic powder penetrating these gaps. The SLM specimens in our study did not show a laminated structure. This may be because the lamination thickness in the laser irradiation was set at a low thickness of 25 μm, whereas the Al_2O_3 used for airborne-particle abrasion had a large particle size of 125 μm, allowing the particles to remove the laminated structure. Bae et al[21] also believed that the alloy morphology could depend on the parameters of the SLM process, including the scan speed, particle size, and laser specifications, further affecting the metal-ceramic bond strength.

The cast, milled, and SLM alloys had different metallurgic structures, although they had similar compositions and their metallurgic structures did not differ after porcelain firing. These differences in metallurgic structures imply that the alloys had completely different solidification and/or thermomechanical histories.[31] A precipitated phase appeared in the cast and milled specimens, and a similar result was reported by Al Jabbari et al[15] for a Co-Cr alloy. The metallurgic structure of an alloy affects its corrosion and mechanical properties. SLM produces sintered alloys whose structures have up to 100% nominal density, with a very fine-scale microstructure owing to the local melting and rapid solidification process of the metal powder without a precipitated phase. However, further research is needed to study how different metallurgic structures affect the metal-ceramic bond.

SEM/EDS uses the silicon x-ray count to measure the area of porcelain retained after fracture to evaluate metal-ceramic bond strength. Although here the debonding surfaces of the 3 groups revealed a combination of cohesive and adhesive fracture modes, our SEM/EDS results revealed that the milled and SLM groups had a significantly higher AFAP than that of the cast group. However, the 3-point bending test showed no significant difference among the 3 groups, revealing the discrepancy between the AFAP and bond strength. A similar result was reported by Xiang et al[12] There is no consensus for the best test to evaluate the metal-ceramic bond strength. The 3-point bending test proposed by ISO 9693[22] better simulates clinical conditions, as the specimens are under compression, traction, and shear bond strength simultaneously. Thus, it was a comparatively ideal test to evaluate the metal-ceramic bond strength.

Table 3. AFAP values of cast, milled, and SLM groups

Group	n	Mean ±SD[a]
Cast	10	62.3 ±7.4[a]
Milled	10	80.4 ±3.2[b]
SLM	10	79.2 ±4.0[b]

AFAP, area fraction of adherence porcelain; SLM, selective laser melting. [a]Groups with same superscripted letters not significantly different at α=.05.

Our results show that the milled and SLM metal-ceramic specimens had similar bond strengths to those of the cast specimens and showed better behavior in the porcelain adherence test with a comparable metallurgic structure. Porcelain fracture in metal-ceramic restorations is caused by various factors such as the restoration's structure, the fabrication processes, and the bond between the core and veneering porcelains.[32] The SEM/EDS used are inadequate for measuring the oxide thickness. Thus, to confirm the presence of a sufficiently thick oxide layer on the metal-ceramic restorations fabricated by new techniques, x-ray photoelectron spectroscopy should be used to quantify the oxide thickness and identify the oxide type on the Co-Cr alloy surface. In addition, clinical trials are needed to substantiate the in vitro testing.

CONCLUSIONS

Based on the findings of this in vitro study, the following conclusions were drawn:

1. The metal-ceramic bond strength of Co-Cr alloy is independent of the manufacturing methods.
2. Alloys produced by milling and SLM behave better in the porcelain adherence test.

REFERENCES

1. Walton TR. The up to 25-year survival and clinical performance of 2,340 high gold-based metal-ceramic single crowns. Int J Prosthodont 2013;26:151-60.

2. Ortorp A, Ascher A, Svanborg P. A 5-year retrospective study of cobalt-chromium-based single crowns inserted in a private practice. Int J Prosthodont 2012;25:480-3.
3. van Noort R. The future of dental devices is digital. Dent Mater 2012;28:3-12.
4. Tamac E, Toksavul S, Toman M. Clinical marginal and internal adaptation of CAD/CAM milling, laser sintering, and cast metal ceramic crowns. J Prosthet Dent 2014;112:909-13.
5. Aboushelib MN, Elmahy WA, Ghazy MH. Internal adaptation, marginal accuracy and microleakage of a pressable versus a machinable ceramic laminate veneers. J Dent 2012;40:670-7.
6. Mumtaz KA, Erasenthiran P, Hopkinson N. High density selective laser melting of Waspaloy. J Mater Process Tech 2008;195:77-87.
7. Strub JR, Rekow ED, Witkowski S. Computer-aided design and fabrication of dental restorations: current systems and future possibilities. J Am Dent Assoc 2006;137:1289-96.
8. Miyazaki T, Hotta Y, Kunii J, Kuriyama S, Tamaki Y. A review of dental CAD/CAM: current status and future perspectives from 20 years of experience. Dent Mater J 2009;28:44-56.
9. Kellerhoff RK, Fischer J. In-vitro fracture strength and thermal shock resistance of metal-ceramic crowns with cast and machined Au Ti frameworks. J Prosthet Dent 2007;97:209-15.
10. Ren XW, Zeng L, Wei ZM, Xin XZ, Wei B. Effects of multiple firings on metal-ceramic bond strength of Co-Cr alloy fabricated by selective laser melting. J Prosthet Dent 2016;115:109-14.
11. Xin XZ, Chen J, Xiang N, Wei B. Surface properties and corrosion behavior of Co-Cr alloy fabricated with selective laser melting technique. Cell Biochem Biophys 2013;67:983-90.
12. Xiang N, Xin XZ, Chen J, Wei B. Metal-ceramic bond strength of Co-Cr alloy fabricated by selective laser melting. J Dent 2012;40:453-7.
13. Xin XZ, Xiang N, Chen J, Wei B. In vitro biocompatibility of Co-Cr alloy fabricated by selective laser melting or traditional casting techniques. Mater Lett 2012;88:101-3.
14. Kohorst P, Junghanns J, Dittmer MP, Borchers L, Stiesch M. Different CAD/CAM-processing routes for zirconia restorations: influence on fitting accuracy. Clin Oral Investig 2011;15:527-36.
15. Al Jabbari YS, Koutsoukis T, Barmpagadaki X, Zinelis S. Metallurgical and interfacial characterization of PFM Co-Cr dental alloys fabricated via casting, milling or selective laser melting. Dent Mater 2014;30:79-88.
16. Zeng L, Xiang N, Wei B. A comparison of corrosion resistance of cobalt-chromium-molybdenum metal ceramic alloy fabricated with selective laser melting and traditional processing. J Prosthet Dent 2014;112:1217-24.
17. Joias RM, Tango RN, Junho de Araujo JE, Junho de Araujo MA, Ferreira Anzaloni Saavedra Gde S, Paes-Junior TJ, et al. Shear bond strength of a ceramic to Co-Cr alloys. J Prosthet Dent 2008;99:54-9.
18. Bagby M, Marshall SJ, MarshallS GW Jr. Metal-ceramic compatibility: a review of the literature. J Prosthet Dent 1990;63:21-5.
19. Schweitzer DM, Goldstein GR, Ricci JL, Silva NRFA, Hittelman EL. Comparison of bond strength of a pressed ceramic fused to metal versus feldspathic porcelain fused to metal. J Prosthodont 2005;14:239-47.
20. Serra-Prat J, Cano-Batalla J, Cabratosa-Termes J, Figueras-Alvarez. Adhesion of dental porcelain to cast, milled, and laser-sintered cobalt-chromium alloys: shear bond strength and sensitivity to thermocycling. J Prosthet Dent 2014;112:600-5.
21. Bae EJ, Kim JH, Kim WC, Kim HY. Bond and fracture strength of metal-ceramic restorations formed by selective laser sintering. J Adv Prosthodont 2014;6:266-71.
22. International Organization for Standardization. ISO 9693(E). Metal-ceramic dental restorative systems. 2nd ed. Geneva: International Organization for Standardization; 1999. Available at: http://www.iso.org/iso/store.htm.
23. Oliveira de, Vasconcello LG, Silva LH, Reis DE, Vasconcellos LM, Balducci I, et al. Effect of airborne-particle abrasion and mechanic-thermal cycling on the flexural strength of glass ceramic fused to gold or cobalt-chromium alloy. J Prosthodont 2011;20:553-60.
24. Ringle RD, Macker JR Jr, Fairhurst CW. An x-ray spectrometric technique for measuring porcelain-metal adherence. J Dent Res 1983;62:8933-6.
25. Rathi S, Parkash H, Chittaranjan B, Bhargava A. Oxidation heat treatment affecting metal-ceramic bonding. Indian J Dent Res 2011;22:877-8.
26. Wylie CM, Shelton RM, Fleming GJ, Davenport AJ. Corrosion of nickel-based dental casting alloys. Dent Mater 2007;23:714-23.
27. Wu Y, Moser JB, Jameson LM, Malone WF. The effect of oxidation heat treatment of porcelain bond strength in selected base metal alloys. J Prosthet Dent 1991;66:439-44.
28. Johnson T, Van Noort R, Stokes CW. Surface analysis of porcelain fused to metal systems. Dent Mater 2006;22:330-7.
29. Akova T, Ucar Y, Balkaya MC, Brantley WA. Comparison of the bond strength of laser-sintered and cast base metal dental alloys to porcelain. Dent Mater 2008;24:1400-4.
30. Lee DH, Lee BJ, Kim SH, Lee KB. Shear bond strength of porcelain to a new millable alloy and a conventional castable alloy. J Prosthet Dent 2015;113:329-35.
31. Yoda K, Suyalatu, Takaichi A, Nomura N, Tsutsumi Y, Doi H, et al. Effects of chromium and nitrogen content on the microstructures and mechanical properties of as-cast Co-Cr-Mo alloys for dental applications. Acta Biomater 2012;8:2856-62.
32. Benetti P, Della Bona A, Kelly JR. Evaluation of thermal compatibility between core and veneer dental ceramics using shear bond strength test and contact angle measurement. Dent Mater 2010;26:743-50.

Corresponding author:
Dr Jiantao Ye
Sun Yat-Sen Memorial Hospital
Sun Yat-Sen University
Guangzhou
PR CHINA
Email: dutaoye@163.com

Acknowledgments
The authors thank technical director Ruinan Li for assistance with specimen fabrication.